CHEMISTRY
A EUROPEAN JOURNAL

DOI: 10.1002/chem.200701945

Self-Assembled Double-Shelled Ferrihydrite Hollow Spheres with a Tunable Aperture

Zhengcui Wu,[a, b] Miao Zhang,[a] Kuai Yu,[a] Shudong Zhang,[a] and Yi Xie*[a]

Abstract: Novel double-shelled hierarchical ferrihydrite hollow spheres ($Fe_{10}O_{14}(OH)_2{\cdot}4H_2O$) were successfully synthesized on a large scale by using a facile medicine-inspired solution-phase approach. Sodium nitroprusside (SNP), an ordinary and inexpensive medicine for expanding blood vessels, served as both a ferric source and an in situ formed gas-bubble template with the presence of sodium dihydrogen phosphate as a pH regulator, coordinator, and stabilizer. A twice-gas-bubble template model has been proposed for the formation of the double-shelled hollow spheres to take advantage of the dissociation and hydrolyzation of the two kinds of ligands in the SNP precursor. The size of the double-shelled ferrihydrite hollow spheres can be tuned by varying the experimental parameters. As-obtained ferrihydrite is highly sensitive to ethanol gas, which indicates potential applications in the field of sensing devices.

Keywords: iron · mesoporous materials · self-assembly · sensors · synthesis design

Introduction

Ferrihydrite is a common, naturally occurring iron oxide material found in aquatic systems and soils,[1–3] and is routinely used in a variety of industrial applications, such as direct coal liquefaction and metallurgical processing.[4,5] It is an environmentally important nanocrystalline phase, which can act as a scavenger for numerous natural and anthropogenic chemical species, including heavy metals[6] and arsenate[7] through adsorption and coprecipitation, and can participate in redox reactions.[8] It is also suspected to constitute the inorganic core of ferritin, an iron storage protein that plays a key role in controlling the levels of iron in plants, animals, and microbes, thereby providing a fully biocompatible material to carry iron particles in potential drug delivery applications.[9] The important applications of ferrihydrite make it widely studied and readily synthesized artificially; however, to date, only nanocrystals of less than 10 nm were usually obtained.[10,11] Because of its nanocrystalline nature and poor crystallinity, the exact structure of ferrihydrite has remained controversial until very recently Michel et al. applied a synchrotron radiation technique and the atomic pair distribution function (PDF) method to ferrihydrite, and revealed that this particular structure contains 20% tetrahedrally and 80% octahedrally coordinated iron in its ideal form and has a basic structural motif closely related to the Baker–Figgis δ-Keggin cluster.[10]

Self-assembled hierarchical structures with hollow interiors have been receiving much attention recently because they could be used to find new applications owing to their conspicuous physicochemical properties that differ markedly from those of nonhollow materials. Various methodologies have been developed to achieve this special nano- and submicrostructure including template and template-free approaches. Generally, however, only single-shelled hollow spheres are obtained. Recently, double-shelled or multishelled hollow spheres using a hard template (hollow latex, polymer spheres, or inorganic silica),[12] soft template (surfactant-molecule vesicles),[13] or an intermediate-templating phase-transformation process[14] have been synthesized. But the synthesis of double-shelled or multishelled hollow-structured materials with a tunable size through the use of an easy one-step solution-phase route still remains a huge technological challenge.

[a] Dr. Z. Wu, M. Zhang, K. Yu, S. Zhang, Prof. Dr. Y. Xie
Department of Nanomaterials and Nanochemistry
Hefei National Laboratory for Physical Sciences at Microscale
University of Science and Technology of China
Hefei, Anhui 230026 (China)
Fax: (+86) 551-360-3987
E-mail: yxie@ustc.edu.cn

[b] Dr. Z. Wu
Anhui Key Laboratory of Functional Molecular Solids
College of Chemistry and Materials Science
Anhui Normal University, Wuhu 241000 (China)

Supporting information for this article is available on the WWW under http://www.chemeurj.org/ or from the author.

Sodium nitroprusside (SNP), an inexpensive medicine, is widely used for the emergency treatment of high blood pressure (hypertensive crisis) and severe heart failure to reduce heart workload. It is also used to produce controlled hypotension (low blood pressure) in anesthetized patients during surgery. The pharmacological effect of SNP is that it serves as a source of nitric oxide, a potent peripheral vasodilator that affects both arterioles and venules. This release of NO gas gives us a clue that SNP can be not only a cheap ferric precursor, but also an in situ gas-bubble template, because in situ formed gas-bubble templates have been widely used to construct various hollow structures of inorganic materials.[15] More interestingly, an SNP molecule possesses another kind of ligand, a cyano group. Although a cyano group is much more stable in an aqueous solution at room temperature than a nitroso group, it is well-known that cyano ions can be released under hydrothermal conditions and subsequently hydrolyze into $HCOO^-$ ions, which can partly hydrolyze into HCOOH and further decompose to CO gas given suitable conditions. The two kinds of gases may form at different reaction stages due to the different dissociation and hydrolyzation sequences of the ligands in the precursor, which affords a good opportunity to construct a complex hollow structure. Motivated by this potential, we successfully synthesized double-shelled ferrihydrite hollow spheres through using the hydrolyzation of SNP in the presence of sodium dihydrogen phosphate. SNP served as both a ferric source and a twice-gas-bubble template, providing not only nitric oxide for the inner-shelled hollow structure but also carbon monoxide for the outer-shelled hollow configuration. This method to build a double-shelled hollow hierarchy spontaneously in a synthetic process is an undoubtedly inexpensive, simple, and efficient approach for the high-throughput production of multishelled hollow spheres. The impact could be tremendous. Furthermore, double-shelled hollow spheres of ferrihydrite with different sizes can be fabricated by varying the experimental parameters, which is very attractive for practical applications. More importantly, our approach offers the first opportunity to investigate the application of ferrihydrite in gas sensing. The high sensitivity to ethanol makes ferrihydrite an alternative material for gas sensing, thereby extending the application fields of ferrihydrite.

Results and Discussion

The morphology of the products was characterized by transmission electron microscopy (TEM). As shown in Figure 1a and b, a strong contrast between the dark edges and the pale center confirms that all of the spherical particles have a hollow cavity. The detailed image reveals the fact that almost all particles are double-shelled hollow structures, as can be clearly seen from the higher magnification TEM image in Figure 1b. The sizes of the double-shelled hollow spheres, the inner hollow spheres, and the inner pores are estimated to be about 300, 190, and 110 nm, respectively.

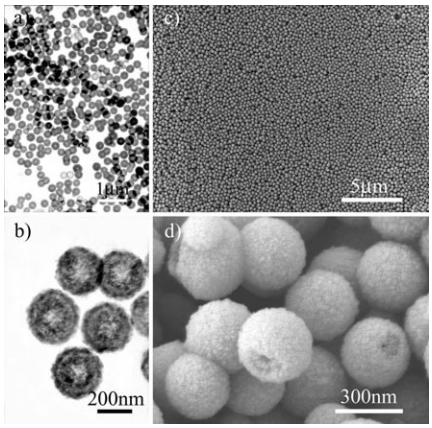

Figure 1. Typical TEM and FESEM images of the as-obtained ferrihydrite double-shelled hollow spheres prepared from SNP (0.5 mmol) and $NaH_2PO_4 \cdot 2H_2O$ (0.19 mmol) in water (40 mL) at 180 °C for 12 h. a) TEM image at a low magnification, indicating that the double-shelled hollow spheres can be fabricated on a large scale. b) TEM image at a high magnification, clearly showing the hollow spheres were double-shelled. c) FESEM image at low magnification, further reflecting the large production and good uniformity of the double-shelled hollow spheres. d) FESEM image at high magnification. The double-shelled structure can be deduced from the broken spheres.

The low-magnification field-emission scanning electron microscopy (FESEM) image shown in Figure 1c indicates that the as-prepared sample is highly uniform and in large production, and the double-shelled structure is further confirmed by the higher magnification FESEM image of the cracked hollow spheres, as shown in Figure 1d. The XRD pattern (Figure S1 in the Supporting Information) shows that the as-prepared sample is a poorly crystallized material and corresponds to a six-line ferrihydrite phase.[1,11a,16]

X-ray photoelectron spectroscopy (XPS) was applied to characterize the surface electronic structure and the chemical element valence by referencing the C 1s line to 284.5 eV. The survey XPS spectrum reveals that the product contains Fe and O (Figure 2a), and there are two weak peaks for P 2s and P 2p in this XPS spectrum, which could be attributed to the surface adsorption of phosphate ions.[17,18] The high-resolution XPS Fe 2p spectrum in Figure 2b shows two distinct peaks at binding energies of ≈710.9 eV for Fe $2p^3/_2$ and ≈724.3 eV for Fe $2p^1/_2$ with a shake-up satellite at ≈719.3 eV, which is characteristic of Fe^{3+}.[18]

To analyze the water content in the sample, thermogravimetric analysis (TGA) was carried out in nitrogen. The TGA curve of the sample shows a weight loss of 12.33% related to the procedure of dehydration (Figure 3). The weight loss of 4.13% below 120 °C is normally attributed to the removal of surface-adsorbed water, and the weight loss of 8.20% above 120 °C is believed to correspond to the release of water from the crystals.[11f] Based on the TGA measurement and a recently reported chemical formula,[10] the stoichiometry of the sample is $Fe_{10}O_{14}(OH)_2 \cdot 4H_2O$. The content of Fe in the product, determined by inductively coupled plasma (ICP) spectrometry, is 59.8%, which is close to the value of 62.9%, calculated according to the stoichiometry.

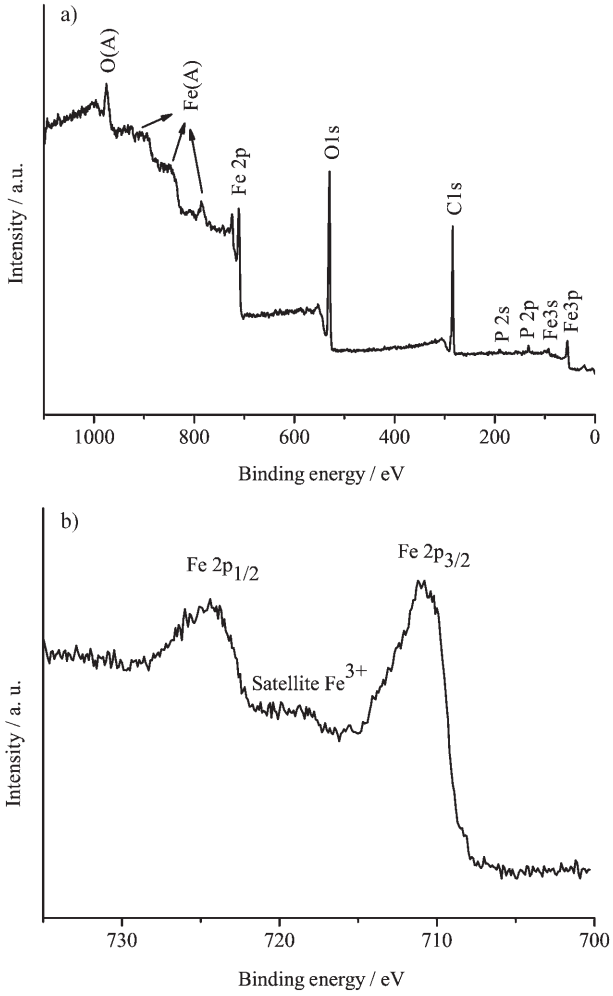

Figure 2. a) Survey XPS spectrum of the double-shelled ferrihydrite hollow spheres sample. (A) represents the auger peak of the corresponding chemical element. b) High-resolution XPS Fe 2p spectrum.

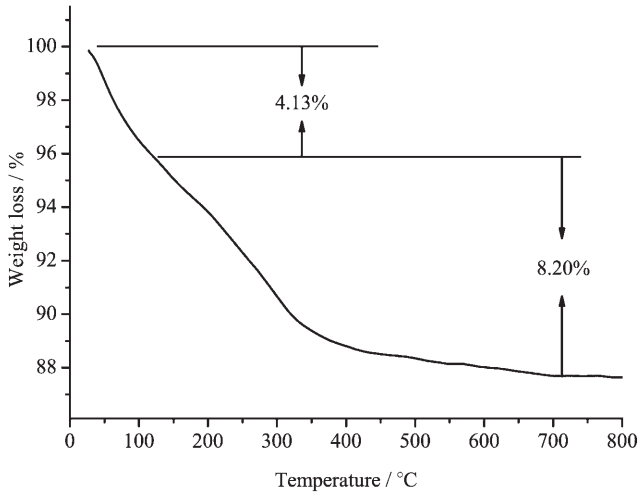

Figure 3. TGA curve of the double-shelled ferrihydrite hollow spheres sample.

Such double-shelled hollow spheres possess a mesoporous structure, as evidenced by the nitrogen-sorption experiment (Figure 4). The isotherm of the sample can be categorized as

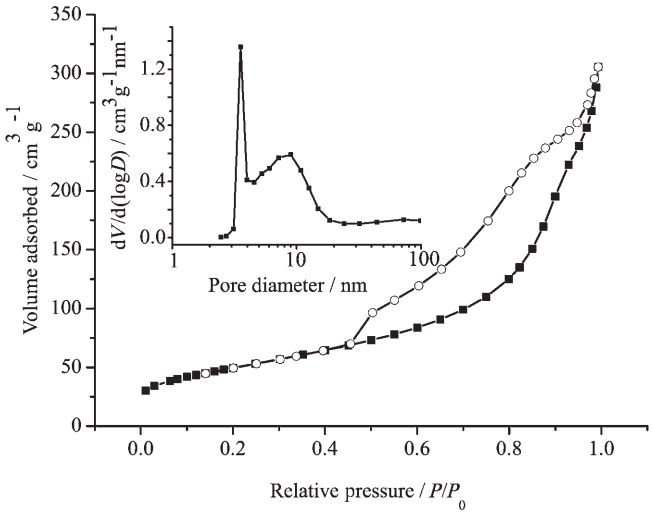

Figure 4. Nitrogen adsorption–desorption (■: adsorbed, ○: desorbed) isotherm of the double-shelled ferrihydrite hollow spheres sample. The inset is its BJH pore-size distribution curve.

type IV, with a distinct hysteresis loop observed in the range 0.45–1.0 P/P_0. The measurement shows that the Brunauer–Emmett–Teller (BET) surface area is 177.9 $m^2 g^{-1}$ and that there are two porous central distributions, one at 3.6 nm, the other at 8.6 nm (Figure 4, inset), which may be due to irregular packing of small crystallites. Such a porous structure provides efficient transport pathways to their interior voids, which is critical for delivery, catalyst, and other applications.[19]

To understand the growth mechanism of the double-shelled ferrihydrite hollow spheres accurately, it is necessary to investigate the morphology evolution of the intermediates involved in the formation. Three intermediates caught at 2, 3, and 4 h showed that single-shelled spheres formed first and were then covered with an outer shell to form double-shelled hollow spheres (Figure S2-1 in the Supporting Information). This process was clearly related to the hydrolyzation of SNP, in which two kinds of ligands (cyano and nitroso groups) in its structure might have a special role in the construction of the isotropic double-shelled hollow structure of ferrihydrite. Under hydrothermal conditions, ferrihydrite building clusters were generated through the hydrolyzation of SNP accompanied by the simultaneous release of NO gas, which functioned as the gas-bubble template and aggregation center for the formation of single-shelled hollow spheres. As-formed single-shelled hollow spheres contained a large number of hydrolyzable ligands (e.g., −CN and −COOH), possibly due to slow reaction kinetics[19] caused by the adsorption of phosphate ions. As the reaction time increased, $HCOO^-$ ions on the surface of single-shelled hollow spheres increased as more cyano groups hydrolyzed

and gradually migrated to the outer surface of the hollow spheres due to their hydrophilicity. As some of the $HCOO^-$ ions were further hydrolyzed into HCOOH, CO gas was then released from the decomposition of HCOOH at elevated temperature, which served as the second gas template for the growth of the outer shell of the double-shelled hollow spheres. Thus, a twice-gas-bubble template model was proposed for the formation of double-shelled hollow spheres, as shown in Scheme 1. Interestingly, as the reaction time was

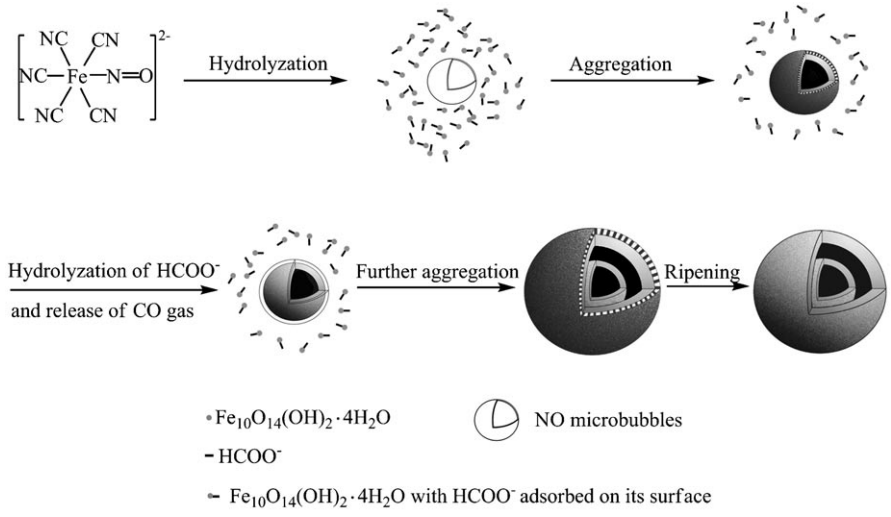

Scheme 1. Proposed growth process of double-shelled ferrihydrite hollow spheres by using a twice-gas-bubble approach.

increased to 18 h, these double-shelled hollow spheres gradually changed into single-shelled hollow spheres with a size of about 280 nm, which were even stable after 114 h (Figure S2-1 in the Supporting Information). The evolution of the ferrihydrite morphology with the reaction time suggested that the whole growth process was a kinetic and thermodynamic competition process; that double-shelled hollow spheres were kinetically favored in a certain middle reaction stage; and that with further aging, the nanocrystallites at the inner shell were thermodynamically driven to relocate themselves to the outer shell because of the higher surface energy during Ostwald ripening.[20] The intermediates at different reaction stages were all determined as six-line ferrihydrite by XRD characterization (Figure S2-2 in the Supporting Information). The Fourier transform infrared (FTIR) spectrum of the product from the upper solution, which had been evaporated under reduced pressure, confirmed the formation of formate in the hydrolyzed products of SNP (Figure S3-1 in the Supporting Information), and the reaction equations are summarized in Figure S3-2 in the Supporting Information. Furthermore, our comparative experiments (Figure S3-3 in the Supporting Information) demonstrated that the formation of the twice-gas-bubble template was clearly related to the concentration of $NaH_2PO_4{\cdot}2H_2O$, which affected the kinetic process of the hydrolytic abilities of the double ligands in the precursor. All of the above supplemental results provide strong support to the proposed mechanism.

More interestingly, our experiments also provide fundamental evidence that the existence of $NaH_2PO_4{\cdot}2H_2O$ is also critical for the formation of a ferrihydrite phase. Only α-Fe_2O_3 micropine dendrites were obtained without sodium dihydrogen phosphate, even at the same initial pH value with the existence of acetic acid or hydrosulfate sodium (Figure S4 in the Supporting Information). These results imply that sodium dihydrogen phosphate not only serves as a pH regulator, but also plays other more important roles. It is well-known that the hydrolysis of ferric ions can produce various iron oxides and iron oxyhydroxides under different conditions.[21] In our case, the hydrolyzation and the following condensation of ferric ions are responsible for the formation of the FeO_6 octahedra with either vertex sharing or edge sharing in the final ferrihydrite structure. Meanwhile, the coordination of phosphate ions to ferric ions prevents the further condensation of the ferric complex at two chelate positions. This results in the formation of an FeO_4 tetrahedral framework at elevated temperatures due to the removal of the hydrophosphate groups, with the hydroxyl groups helping to balance the framework charges. As one might expect, FeO_4 tetrahedra tend to only share corners with other FeO_6 octahedra to diminish the instability[22] in the final ferrihydrite structure (Figure 5a). Thus, the presence of $NaH_2PO_4{\cdot}2H_2O$ plays a critical role in the formation of the particular ferrihydrite structure consisting of 20% FeO_4 and 80% FeO_6 polyhedra in its ideal form.[10] Simultaneously, the existence of phosphate ions may also be important to stabilize the ferrihydrite phase because phosphate ions can not only cover the surface of ferrihydrite, but also occupy the tunnels of ferrihydrite, which one can clearly see in Figure 5b by comparing the pore size of ferrihydrite (labeled in the top two figures) with the size of the hydrophosphate ion (labeled in the bottom-right figure). The XPS results also indicate the existence of trace phosphate ions in the final product. It should be mentioned that the hydrophosphate ions were the dominant form that coordinated with ferric ions as the reaction system transformed from weak acidity to alkalescence as the reaction proceeded. (The pH values of the solution before the reaction and the upper solution after the reaction were 5.1 and 9.0, respectively.) The hydrophosphate ions in tunnels are essential in balancing the framework charges and stabilizing the tunnel structure of ferrihydrite, protecting them from aggregation and further conversion to other iron

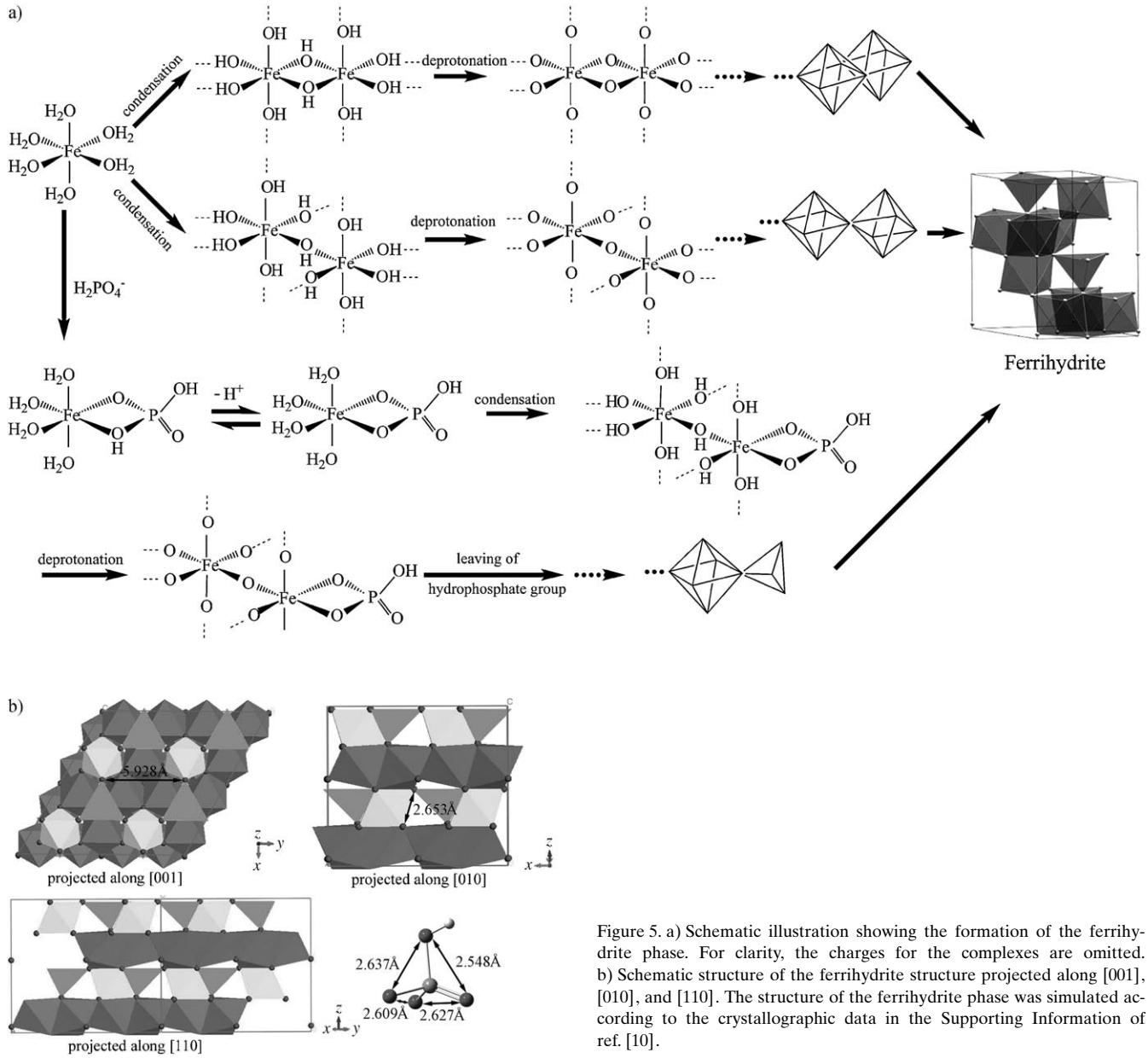

Figure 5. a) Schematic illustration showing the formation of the ferrihydrite phase. For clarity, the charges for the complexes are omitted. b) Schematic structure of the ferrihydrite structure projected along [001], [010], and [110]. The structure of the ferrihydrite phase was simulated according to the crystallographic data in the Supporting Information of ref. [10].

oxides; while a similar effect is also found in akaganeite with the incorporation of F^-, Cl^-, and so forth.[23] Our experiments indicate that the as-prepared ferrihydrite product began the transformation to α-Fe_2O_3 at 700 °C and the complete conversion at 900 °C under N_2 (Figure S5 in the Supporting Information), much higher than that of the unadsorbed ferrihydrite product, which transformed to hematite visibly at 400 °C and completely at 500 °C.[24] The thermostability study confirmed the above conclusion that phosphate ions could help to stabilize the ferrihydrite phase.

The proposed twice-gas-bubble template model also suggests that the size of the double-shelled hollow spheres may be tuned by controlling the kinetic process. The double-shelled hollow spheres with the same outer size, but smaller inner spheres of about 160 nm and smaller inner pores of about 40 nm, were acquired by increasing the reaction temperature to 220 °C with other parameters constant (Figure 6a–c). This indicated that the elevated temperature sped up the reaction and caused ferrihydrite nanoparticles to aggregate on the smaller NO microbubbles, which inhibited them from converging into bigger ones. Also, the release of more CO gas as the second gas-bubble template produced the larger space between the two shells. When the concentration of SNP was increased to 0.84 mmol with other parameters constant, the products were larger double-shelled hollow spheres in which the diameters of outer spheres, inner spheres, and inner pores were about 400, 250, and 130 nm, respectively, as shown in Figure 6d–f. The results

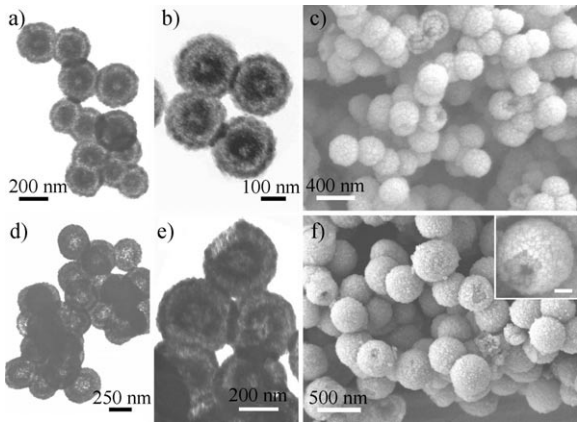

Figure 6. a, b) TEM images and c) FESEM image of the double-shelled ferrihydrite hollow spheres, obtained from SNP (0.5 mmol) and $NaH_2PO_4{\cdot}2H_2O$ (0.19 mmol) at 220 °C. d, e) TEM images and f) FESEM image of the double-shelled ferrihydrite hollow spheres, obtained from SNP (0.84 mmol) and $NaH_2PO_4{\cdot}2H_2O$ (0.19 mmol) at 180 °C. The inset in Figure 6f is the magnified FESEM image of an individual double-shelled hollow sphere (scale bar: 100 nm).

demonstrate that the slight variations in reaction conditions within the stability field of a precipitate affect the size and morphology of the products remarkably.

To expand the applied range of ferrihydrite, we researched the potential application of ferrihydrite in gas sensing on account of its innate characteristics as a metal oxide semiconductor. The sensing properties of the products towards trace levels of gas were analyzed at room temperature in dry air. The gas sensitivity is defined as the resistance ratio R_{air}/R_{gas}, in which R_{air} and R_{gas} are the electrical resistances for sensors in air and in gas, respectively. Figure 7 shows the room-temperature gas-sensing behavior of the as-synthesized double-shelled hollow spheres in response to ethanol compared with single-shelled hollow spheres (Figure S3-3a in the Supporting Information). The sensitivity of the products increases with an increase of ethanol gas concentration. However, the single-shelled hollow spheres are less sensitive. The gas sensitivity of double-shelled hollow spheres is observed even at a concentration of 10 ppm, which indicates its potential application in gas detection. We have also found that the on and off responses for the products could be repeated many times without observing major changes in the signal, thereby illustrating favorable reversibility. The double-shelled hollow spheres have larger surface areas than single-shelled hollow spheres (with BET surface area 102.5 $m^2 g^{-1}$), and the higher sensitivity is attributed to the double-shelled structure of the sample, which provides more space and active sites for adsorption and desorption of gas molecules. It is generally accepted that materials with high surface areas are advantageous for obtaining a high sensitivity in sensing applications.[25]

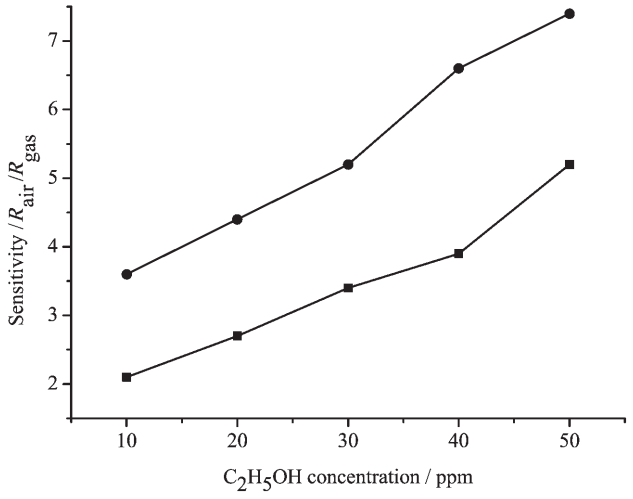

Figure 7. Room-temperature sensitivity of the sensors made of as-prepared double-shelled (●) and single-shelled (■) ferrihydrite hollow spheres to ethanol. The gas sensitivity is defined as the resistance ratio R_{air}/R_{gas}, in which R_{air} and R_{gas} are the electrical resistances for sensors in air and in gas, respectively.

Conclusion

In summary, we describe a facile, one-step, surfactant-free, solution-phase route, based on a twice-gas-bubble template model to produce double-shelled ferrihydrite hollow spheres with a tunable aperture. In this self-assembly process, SNP possesses two kinds of ligands and serves as not only a ferric source, but also an important in situ twice-gas-bubble template for the formation of the double-shelled hollow structure. The presence of phosphate in this process also plays a multiple role, not only as the pH regulator, but also as the coordinator and stabilizer for the particular ferrihydrite phase. Importantly, this material exhibits high sensitivity in gas sensing, which could be of great importance in extending the potential applications of ferrihydrite. This work provides a novel pathway to synthesize double-shelled hollow microstructures of inorganic compounds, offering a new material platform for delivery carriers, catalysts, and other applications.

Experimental Section

General: In a typical experimental procedure, sodium nitroprusside (SNP, $Na_2[Fe(CN)_5NO]{\cdot}2H_2O$; 0.5 mmol) was dissolved in distilled water (40 mL) in a Teflon-lined autoclave, and sodium dihydrogen phosphate ($NaH_2PO_4{\cdot}2H_2O$; 0.19 mmol) was added. The autoclave was sealed, heated at 180 °C for 12 h, and allowed to cool to room temperature naturally. The precipitate was collected by centrifugation and washed with distilled water and ethanol several times, and then dried in a vacuum at 50 °C for 10 h.

The structure of these obtained samples was characterized by using the XRD pattern, which was recorded on a Rigaku Dmax diffraction system with monochromatized $Co_{K\alpha}$ radiation. The TEM images were obtained by using a Hitachi 800 system at 200 kV. The SEM images were taken by using a JEOL JSM-6700F field-emission scanning electron microscope (20 kV). XPS analysis of the product was performed by using an ESCALAB MK II X-ray photoelectron spectrometer and non-monochromat-

ized Al–$Mg_{K\alpha}$ X-rays as the excitation source. TGA of the as-synthesized sample was carried out on a Shimadzu TA-50 thermal analyzer at a heating rate of 10 K min^{-1} from room temperature to 800 °C under nitrogen. The content of Fe was determined by using Optima 5300DV inductively coupled plasma spectrometry. BET nitrogen adsorption–desorption was measured by using a Micromeritics ASAP 2020 accelerated surface area and porosimetry system. The pH value was determined on a Delta 320 pH meter (Mettler-Toledo Instrument Co.).

Sensing tests: The sensing tests were carried out by using the as-prepared model sensors. The sample was mixed with several drops of ethanol to form a homogeneous slurry, and was then coated on the interdigital electrode and the electrode was dried in a vacuum at 50 °C for 3 h. The optical digital photograph of the interdigital electrode is shown in Figure S6 in the Supporting Information. Measurements were performed by using a WS-30A system at room temperature (Weisheng Instruments Co., Zhengzhou, China).

Acknowledgements

This work was financially supported by the National Natural Science Foundation of China (no. 20621061) and the State Key Project of Fundamental Research for Nanomaterials and Nanostructures (2005CB623601).

[1] J. L. Jambor, J. E. Dutrizac, *Chem. Rev.* **1998**, *98*, 2549–2585.
[2] D. G. Rancourt, D. Fortin, T. Pichiler, P. J. Thibault, G. Lamarche, R. V. Morris, P. H. J. Mercier, *Am. Mineral.* **2001**, *86*, 834–851.
[3] U. Schwertmann, L. Carlson, E. Murad, *Clays Clay Miner.* **1987**, *35*, 297–304.
[4] G. P. Huffman, B. Ganguly, J. M. Zhao, K. R. P. M. Rao, N. Shah, Z. Feng, F. E. Huggins, M. M. Taghiei, F. L. Lu, *Energy Fuels* **1993**, *7*, 285–296.
[5] P. A. Riveros, J. E. Dutrizac, P. Spencer, *Can. Metall. Q.* **2001**, *40*, 395–420.
[6] R. G. Ford, P. M. Bertsch, K. J. Farley, *Environ. Sci. Technol.* **1997**, *31*, 2028–2033.
[7] K. P. Raven, A. Jain, R. H. Loeppert, *Environ. Sci. Technol.* **1998**, *32*, 344–349.
[8] D. Fortin, S. Langley, *Earth Sci. Rev.* **2005**, *72*, 1–19.
[9] a) A. Lewin, G. R. Moore, N. E. Le Brun, *Dalton Trans.* **2005**, *22*, 3597–3610; b) H. Pardoe, W. Chua-anusorn, T. G. St Pierre, J. Dobson, *Phys. Med. Biol.* **2003**, *48*, N89–N95.
[10] F. M. Michel, L. Ehm, S. M. Antao, P. L. Lee, P. J. Chupas, G. Liu, D. R. Strongin, M. A. A. Schoonen, B. L. Phillips, J. B. Parise, *Science* **2007**, *316*, 1726–1729.
[11] a) E. L. Duarte, R. Itri, E. Lima, Jr., M. S. Baptista, T. S. Berquó, G. F. Goya, *Nanotechnology* **2006**, *17*, 5549–5555; b) G. Liu, S. Debnath, K. W. Paul, W. Q. Han, D. B. Hausner, H. A. Hosein, F. M. Michel, J. B. Parise, D. L. Sparks, D. R. Strongin, *Langmuir* **2006**, *22*, 9313–9321; c) Y. Guyodo, S. K. Banerjee, R. L. Penn, D. Burleson, T. S. Berquo, T. Seda, P. Solheid, *Phys. Earth Planet. Inter.* **2006**, *154*, 222–233; d) N. J. O. Silva, V. S. Amaral, V. D. Z. Bermudez, S. C. Nunes, D. Ostrovskii, J. Rocha, L. D. Carlos, *J. Mater. Chem.* **2005**, *15*, 484–490; e) V. Barrón, J. Torrent, E. D. Grave, *Am. Mineral.* **2003**, *88*, 1679–1688; f) F. M. Michel, L. Ehm, G. Liu, W. Q. Han, S. M. Antao, P. J. Chupas, P. L. Lee, K. Knorr, H. Eulert, J. Kim, C. P. Grey, A. J. Celestian, J. Gillow, M. A. A. Schoonen, D. R. Strongin, J. B. Parise, *Chem. Mater.* **2007**, *19*, 1489–1496.
[12] a) M. Yang, J. Ma, Z. W. Niu, X. Dong, H. F. Xu, Z. K. Meng, Z. G. Jin, Y. F. Lu, Z. B. Hu, Z. Z. Yang, *Adv. Funct. Mater.* **2005**, *15*, 1523–1528; b) M. Yang, J. Ma, C. L. Zhang, Z. Z. Yang, Y. F. Lu, *Angew. Chem.* **2005**, *117*, 6885–6888; *Angew. Chem. Int. Ed.* **2005**, *44*, 6727–6730; c) X. W. Lou, C. L. Yuan, L. A. Archer, *Small* **2007**, *3*, 261–265.
[13] H. L. Xu, W. Z. Wang, *Angew. Chem.* **2007**, *119*, 1511–1514; *Angew. Chem. Int. Ed.* **2007**, *46*, 1489–1492.
[14] H. G. Zhang, Q. S. Zhu, Y. Zhang, Y. Wang, L. Zhao, B. Yu, *Adv. Funct. Mater.* **2007**, *17*, 2766–2771.
[15] a) C. Z. Wu, Y. Xie, L. Y. Lei, S. Q. Hu, C. Z. OuYang, *Adv. Mater.* **2006**, *18*, 1727–1732; b) X. X. Li, Y. J. Xiong, Z. Q. Li, Y. Xie, *Inorg. Chem.* **2006**, *45*, 3493–3495; c) L. Guo, F. Liang, X. G. Wen, S. H. Yang, L. He, W. Z. Zheng, C. P. Chen, Q. P. Zhong, *Adv. Funct. Mater.* **2007**, *17*, 425–430; d) Y. S. Han, G. Hadiko, M. Fuji, M. Takahashi, *Chem. Lett.* **2005**, *34*, 152–153; e) C. L. Jiang, W. Q. Zhang, G. F. Zou, W. C. Yu, Y. T. Qian, *Nanotechnology* **2005**, *16*, 551–554; f) Q. Peng, Y. J. Dong, Y. D. Li, *Angew. Chem.* **2003**, *115*, 3135–3138; *Angew. Chem. Int. Ed.* **2003**, *42*, 3027–3030; g) J. Zhang, L. D. Sun, C. S. Liao, C. H. Yan, *Chem. Commun.* **2002**, *3*, 262–263.
[16] a) R. A. Eggleton, R. W. Fitzpatrick, *Clays Clay Miner.* **1988**, *36*, 111–124; b) K. M. Towe, W. F. Bradley, *J. Colloid Interface Sci.* **1967**, *24*, 384–392; c) V. A. Drits, B. A. Sakharov, A. L. Salyn, A. Manceau, *Clay Miner.* **1993**, *28*, 185–207.
[17] C. J. Jia, L. D. Sun, Z. G. Yan, L. P. You, F. Lou, X. D. Han, Y. C. Pang, Z. Zhang, C. H. Yan, *Angew. Chem.* **2005**, *117*, 4402–4407; *Angew. Chem. Int. Ed.* **2005**, *44*, 4328–4333.
[18] X. L. Hu, J. C. Yu, J. M. Gong, Q. Li, G. S. Li, *Adv. Mater.* **2007**, *19*, 2324–2329.
[19] H. X. Li, Z. F. Bian, J. Zhu, D. Q. Zhang, G. S. Li, Y. N. Huo, H. Li, Y. F. Lu, *J. Am. Chem. Soc.* **2007**, *129*, 8406–8407.
[20] a) Y. Chang, J. J. Teo, H. C. Zeng, *Langmuir* **2005**, *21*, 1074–1079; b) H. G. Yang, H. C. Zeng, *J. Phys. Chem. B* **2004**, *108*, 3492–3495; c) J. Li, H. C. Zeng, *Angew. Chem.* **2005**, *117*, 4416–4419; *Angew. Chem. Int. Ed.* **2005**, *44*, 4342–4345.
[21] C. M. Flynn, Jr., *Chem. Rev.* **1984**, *84*, 31–41.
[22] L. Pauling, *J. Am. Chem. Soc.* **1929**, *51*, 1010–1026.
[23] a) J. E. Post, V. F. Buchwald, *Am. Mineral.* **1991**, *76*, 272–277; b) J. Cai, J. Liu, Z. Gao, A. Navrotsky, S. L. Suib, *Chem. Mater.* **2001**, *13*, 4595–4602.
[24] a) V. Barrón, N. Gálvez, M. F. Hochella, J. Torrent, *Am. Mineral.* **1997**, *82*, 1091–1100; b) A. S. Campbell, U. Schwertmann, P. A. Campbell, *Clay Miner.* **1997**, *32*, 615–622.
[25] a) Y. L. Wang, X. C. Jiang, Y. N. Xia, *J. Am. Chem. Soc.* **2003**, *125*, 16176–16177; b) C. J. Martinez, B. Hocky, C. B. Montgomery, S. Semancik, *Langmuir* **2005**, *21*, 7937–7944; c) Q. R. Zhao, Y. Gao, X. Bai, C. Z. Wu, Y. Xie, *Eur. J. Inorg. Chem.* **2006**, 1643–1648; d) Y. Zhao, Y. Xie, X. Zhu, S. Yan, S. X. Wang, *Chem. Eur. J.* **2008**, *14*, 1601–1606.

Received: December 8, 2007
Published online: April 23, 2008

